Synchronous Tracking Control of Parallel Manipulators Using Cross-coupling Approach

D. Sun, R. Lu, J. K. Mills and C. Wang

The International Journal of Robotics Research 2006; 25; 1137

DOI: 10.1177/0278364906072037

D. Sun
Department of Manufacturing Engineering and Engineering Management
City University of Hong Kong
Kowloon, Hong Kong
medsun@cityu.edu.hk

R. Lu
J. K. Mills
Department of Mechanical and Industrial Engineering
University of Toronto
Toronto, ON M5S 3G8 Canada
ren@mie.utoronto.ca
mills@mie.utoronto.ca

C. Wang
Department of Manufacturing Engineering and Engineering Management
City University of Hong Kong
Kowloon, Hong Kong
cwang2@cityu.edu.hk

Synchronous Tracking Control of Parallel Manipulators Using Cross-coupling Approach

Abstract

This paper presents a cross-coupled control approach to the tracking control of parallel manipulators in a synchronous manner. Based on the synchronization goal, the position synchronization error is investigated by considering motion synchronization between each actuator joint and its adjacent ones. A decentralized trajectory tracking controller is then developed with feedback of both position and synchronization errors, formed with a combination of feedforward, feedback and a saturation control. It is proven that this tracking controller can asymptotically stabilize both position and synchronization errors of the system. The proposed controller does not require the explicit use of the system dynamic model. Experiments performed on a 3-DOF parallel manipulator demonstrate improved performance with the proposed synchronous control design.

KEY WORDS—Cross-coupled control, parallel manipulators, synchronization, trajectory tracking

The International Journal of Robotics Research
Vol. 25, No. 11, November 2006, pp. 1137-1147
DOI: 10.1177/0278364906072037

1. Introduction

Due to their advantages of high stiffness, high accuracy, and high load-carrying capacity, parallel robotic manipulators have been widely used in various industrial applications, such as flight simulation (Stauffer 1984), precision machining (Chen and Song 1994), telescopes (Carretero et al. 1998), and high speed assembly operations (Clavel 1998). The majority of the parallel manipulators studied are fully parallel manipulators in which the number of chains is strictly equal to the number of degrees of freedom (DOF) of the manipulator end-effector. Fully parallel manipulators can be classified into two main categories: planar parallel manipulators, which have three DOF in the plane, and spatial parallel manipulators, which move out of the plane (Merlet 2000).

Various control strategies have been proposed to solve the control problem of fully parallel robots. Independent joint controllers (i.e., PD or PID type) are usually employed in industrial robot manipulators (Amirat et al. 1996) because they do not require the explicit use of the system dynamic model. However, these simple controllers exhibit inherently low rejection to exogenous disturbances. Chiacchio et al. (1993) proposed a linear control scheme, in which an acceleration feedback term is used making the control law more robust to exogenous disturbances than a simple PID. Other non-model based controls include fuzzy logic control (Begon et al. 1995) and neural network control (Pernechele et al. 2000). Various model-based control design methods, which compensate for the available estimates of the dynamic parameters in a feedback or in a feedforward fashion, have been proposed. With an outer feedback loop, these approaches provide robustness to imperfect modeling and disturbances. The computed-torque control (Kokkinis and Stoughton 1996) is the pioneer design of this kind. A large number of control methods, for example, the sliding mode method (Park et al. 2001), impedance control (Fasse and Gosselin 1999), and adaptive control (Sirouspour and Salcudean 2001; Lin and McInroy 2003), are categorized within this class of controllers as well. In order to improve tracking performance further, motivated by a dynamic model with unknown parameters, many control schemes consisting of several combined control methods have been proposed for fully parallel robots. For example, a control that combines cascaded cerebellar model articulation control with variable structure control (Li et al. 2002), a neural-net tuned PID control method (Karkoub et al. 2004), a neural-fuzzy method (Nefti et al. 2002), and many other approaches.

Characterizing the majority of traditional parallel manipulator controllers, the control loop of an individual actuator receives only local feedback information from the controlled joint, and no feedback from other joints associated with the remaining actuators. Hence, disturbances in the control loop of one actuator cause an error that is corrected by this loop only, while the others do not respond. Since the trajectory of the end-effector is determined by all actuator motions, all actuated joints in the manipulator should be controlled in a synchronous manner so that a pre-determined trajectory can be followed with high tracking accuracy. Otherwise, tracking accuracy will be reduced due to uncoordinated motions of the actuated joints. In some severe situations, for instance, when accelerations of actuated joints are high, damage to the manipulator mechanical structure may occur.

Cross-coupling control (Koren 1980) provides a unique advantage and opportunity to solve the synchronized control problem posed by parallel manipulators. Over the past decade, cross-coupling technology has been applied mainly to machine tools (Kulkarni and Srinivasan 1990; Tomizuka et al. 1992; Koren and Lo 1992). Much of the reported research dealt with the velocity synchronization problem, especially for two-axis motions. Recently, great progress has been made in utilizing the cross-coupling concept to solve position synchronization of multiple motion axes (Chiu and Tomizuka 1998; Sun 2003). In robotics, cross-coupling technology has been used for mobile robot control (Feng et al. 1993; Sun et al. 2005; Borenstein 1995) and coordination of robot manipulators (Sun and Mills 2002; Naumovic 1999; Rodriguiz-Angeles and Nijmeijer 2004; Chuang and Chang 2000). Other synchronization control approaches include fuzzy logic coupling control (Moore and Chen 1995), neuro-controller for synchronization (Lee and Jeon 1998), and linear quadratic optimal control (McNab and Tsao 2000). The synchronization scheme was also applied in a distributed computing system, i.e., "tight" and "loose" couplings (Gauthier et al. 1987). It has been shown that adaptive control is an effective strategy used to address the synchronization problem. An adaptive feedforward controller was first designed and implemented for speed synchronization of two motion axes (Tomizuka et al. 1992), which was followed by Kamano et al. (1993) and Yang and Chang (1996). An adaptive synchronized controller was further developed in Sun (2003) and Sun and Mills (2002), with the advantage that asymptotic convergence of both position tracking and synchronization errors to zero was guaranteed. Some other model-based synchronization controls addressed the contour tracking problem by using implicit representation of curves to model desired contours (Chiu and Tomizuka 1998) and a receding horizon linear quadratic formulation (McNab and Tsao 1994).

It should be noted that most of the existing synchronized controllers reported in the literature are model-based, and of these, some require extensive on-line calculations. In practice, there is significant demand for using non-model based control algorithms, i.e., PID feedback control, leading to significant implementation simplicity. A non-model based variable-gain cross-coupling controller was introduced for a general class of contours (Koren and Lo 1991, 1992). However, the effect of a time-varying gain in the cross-coupling controller on system stability, and the effect of the introduction of time-varying cross-coupling controls on the overall system dynamics have yet to be examined (Chiu and Yomizuku 2001). A control law that consists of a linear time-varying PD error feedback and a linear time invariant trajectory feedforward compensator was proposed by Chiu and Tomizuka (2001), in which the feedforward compensator is calculated from the model dynamics. Another effort to examine the stability and robustness of the cross-coupled control system was reported in Yeh and Hsu (2003).

In this paper, we propose a cross-coupled control approach that does not require the explicit use of the system dynamic model. After defining a synchronization goal, the position synchronization errors are defined as differential position errors of all possible pairs of two neighbor joints. Two of such synchronization errors with adjacent numbers are then combined in integration with the joint position tracking error to form the so-called coupled position error. A tracking controller with feedback of this coupled position error is constructed, as a combination of feedforward/feedback controls and a saturation control. In the following, we prove that the proposed synchronous tracking controller guarantees asymptotic convergence to zero of both position and synchronization errors. Experiments performed on a 3-DOF planar parallel manipulator demonstrate the effectiveness of the proposed approach in performance improvement over non-synchronous controls such as PID feedback.

Compared to many existing synchronous control algorithms, the proposed method is relatively simple in that it does not require the explicit use of the dynamic model. It has long been assumed that the closed kinematic chain of a parallel manipulator creates tight non-linear coupling and requires careful modeling and a model-based approach to achieve the desired performance. The results of this paper support the concept that the performance can be enhanced by using a cross-coupling controller without such system dynamic models.

2. Modeling and Synchronization Error

2.1. Modeling

Figure 1 illustrates a parallel manipulator designed for high-acceleration, high-accuracy electronic component placement or wire bonding tasks. The manipulator has a moving platform, a base platform, and three chains. Each chain is comprised of a prismatic joint and two consecutive revolute joints, with only the prismatic joint actuated. This manipulator is also categorized as P-R-R type, where P and R represent prismatic and revolute joints, respectively.

The three degrees of freedom of the P-R-R manipulator are translations along X and Y axes and rotation about the Z axis, respectively. As shown in Figure 1, the inertial frame (X, Y, Z) is fixed at the center of the base platform with the Z axis directed vertically out of the plane; the mobile frame (X', Y', Z') is fixed at the center of the moving platform with the Z' axis directed vertically out of the plane; (x_P, y_P) are the Cartesian positions of the moving platform at its mass center; ϕ is the orientation of the moving platform with respect to the inertial frame; A_i, B_i are the home and moving positions of the ith prismatic joint, respectively; C_i is the Cartesian position of the terminals of the platform facing the ith intermediate link; ρ_i is the translation distance of the ith prismatic joint; α_i is the constant angle between the X-axis of the inertial frame and the ith linear guide; $i = 1 \cdots n$ ($n = 3$ in Figure 1).

Define a generalized coordinate as $q = \begin{bmatrix} q_1 & \cdots & q_n \end{bmatrix}^T \in \Re^{n\times 1}$, in which q_i denotes the translation of the ith prismatic joint. Denote $X_p \in \Re^{3\times 1}$ as the attitude of the moving platform at its mass center. Using the time derivative of the generalized coordinate and that of the position of the moving platform, we have:

$$\dot{X}_P(t) = (J_P(t))^{-1}\dot{q}(t) \tag{1}$$

where $J_p(t)$ is the Jacobian matrix representing the velocity relationship between the actuated joints and the moving platform.

Using the natural orthogonal complement method, the dynamic model of the P-R-R manipulator is derived as [42]:

$$H(q)\ddot{q}(t) + C(q, \dot{q})\dot{q}(t) = \tau \tag{2}$$

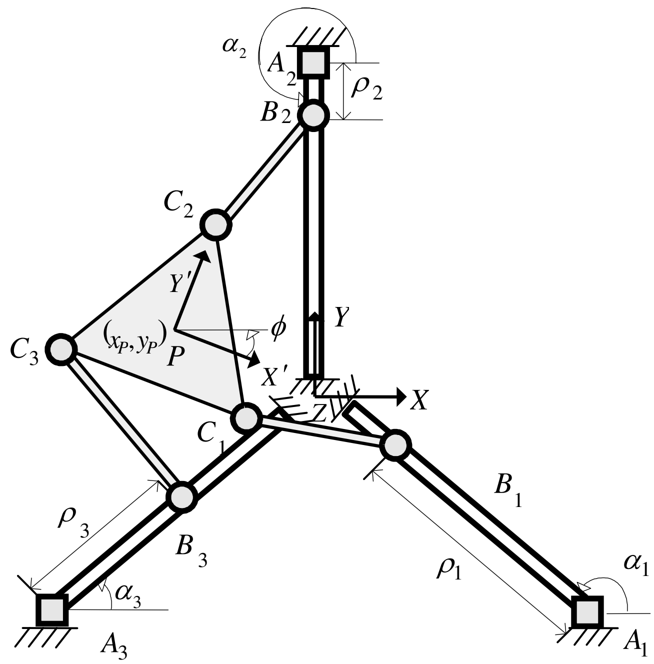

Fig. 1. Coordinate system of the P-R-R manipulator.

where: $H(q) = diag\{H_i(q_i)\} \in \Re^{n\times n}$ is the symmetric, positive-definite inertia matrix; $C(q, \dot{q}) = diag\{C_i(q_i, \dot{q}_i)\} \in \Re^{n\times n}$ is the coefficient matrix of Coriolis and centrifugal forces; $\tau = [\tau_1 \cdots \tau_n]^T \in \Re^{n\times 1}$ is the actuating force exerted on the actuated joints. Note that $\dot{H}(q) - 2C(q, \dot{q})$ is a skew-symmetric matrix.

2.2. Synchronization Error

The essential feature that differentiates synchronized control from conventional PID control is the employment of an additional feedback signal termed the synchronization error. The synchronization errors are typically designed through the combination of position and/or velocity errors of all actuated joints with coupling coefficients. These coupling coefficients are often determined by the kinematic constraints among the actuated joints and consequently are either constant or time-varying (Sun and Mills 2002). The kinematic constraints are derived from the goal of synchronization. As a result, the synchronization error represents the degree of coordination among the actuated joints and is not equivalent to the conventional tracking error. For systems having closed-loop chain structures, employment of the synchronization error provides each actuated joint with motion information both from itself and from the other actuated joints. Such a synchronization error may be determined from kinematic constraints acting on the systems, for example. Hence, the motions of all actuated joints are coordinated and the attitude error of the mobile platform is substantially smaller than that without using the synchronization error. In other words, a synchronous control can achieve better trajectory tracking performance than a conventional non-synchronous control method. This assertion was demonstrated in previous studies (Borenstein and Koren 1987; Sun and Mills 2002).

Define the following equation as the synchronization function that all actuators of the parallel manipulator are required to satisfy simultaneously.

$$f(q_1 \cdots q_n) : s_1 q_1 = s_2 q_2 = \cdots = s_n q_n \tag{3}$$

where s_i denotes the coupling coefficient of the manipulator i and is assumed to be nonzero. This synchronization function actually represents a new task requirement in kinematics. Since eq. (3) holds at all desired coordinates q_i^d, namely

$$f(q_1^d \cdots q_n^d) : s_1 q_1^d = s_2 q_2^d = \cdots = s_n q_n^d \tag{4}$$

we define the following synchronization goal by combining (3) and (4)

$$s_1 \Delta q_1 = s_2 \Delta q_2 = \cdots = s_n \Delta q_n \tag{5}$$

where $\Delta q_i(t) = q_i^d(t) - q_i(t)$ denotes the position error of the prismatic joints, and $q_i^d(t)$ denotes the desired coordinate. Further, the synchronization goal (5) can be divided into n subgoals such as $s_i \Delta q_i = s_{i+1} \Delta q_{i+1}$, with the boundary condition that when $i = n$, $i + 1 = 1$.

We then introduce the concept of position synchronization errors, which are defined as a subset of all possible pairs of two neighboring joints in the following way:

$$\begin{aligned} \varepsilon_1 &= s_1 \Delta q_1 - s_2 \Delta q_2 \\ \varepsilon_2 &= s_2 \Delta q_2 - s_3 \Delta q_3 \\ &\vdots \\ \varepsilon_n &= s_n \Delta q_n - s_1 \Delta q_1 \end{aligned} \tag{6}$$

where ε_i denotes the synchronization error of the joint i. Obviously, if the synchronization error $\varepsilon_i = 0$ for all $i = 1 \sim n$, the synchronization goal (5) can be achieved automatically.

Now, the control objective is to design the actuator inputs to cause $\Delta q_i \to 0$ and $\varepsilon_i \to 0$ as $t \to \infty$. Unlike the traditional non-synchronized control considering the position control only, here the synchronization control between two neighbor manipulators is also required so that (5) holds.

3. Control Design

In this section, a synchronous tracking controller is developed. In a similar way to Sun (2003) and Sun and Mills (2002), we define a coupled position error as

$$e_i = s_i \Delta q_i + \beta \int_0^t (\varepsilon_i - \varepsilon_{i-1})\, dw \tag{7}$$

where β is a positive constant, and w is a variable from time zero to t. ε_i in (7) is subject to the boundary condition that when $i = 1$, $i - 1 = n$. The motivation for such a definition is to ensure both Δq_i and ε_i converge to zero when $e_i \to 0$. It is also noted that the coupled position error e_i of the joint i contains the information of two neighboring joints $i - 1$ and $i + 1$, which can be seen from eq. (7) and the definition of ε_i in (6).

Differentiating e_i with respect to time yields

$$\dot{e}_i = \dot{s}_i \Delta q_i + s_i \Delta \dot{q}_i + \beta (\varepsilon_i - \varepsilon_{i-1}) \tag{8}$$

To construct an asymptotically stable tracking controller to drive $e_i \to 0$ and $\dot{e}_i \to 0$, we utilize Slotine and Li (1987) to introduce a command vector u_i that leads to combined position and velocity errors. Unlike Slotine and Li (1987), here there exists a time-varying coupling parameter s_i in addition to Δq_i in (7). Hence, we may define the command vector u_i as follows:

$$u_i = s_i \dot{q}_i^d + \dot{s}_i \Delta q_i + \beta (\varepsilon_i - \varepsilon_{i-1}) + \Lambda e_i \tag{9}$$

where Λ is a diagonal positive gain matrix. Definition of u_i in (9) leads to the following position/velocity vectors:

$$\begin{aligned} r_i = u_i - s_i \dot{q}_i &= s_i \Delta \dot{q}_i + \dot{s}_i \Delta q_i + \beta (\varepsilon_i - \varepsilon_{i-1}) + \Lambda e_i \\ &= \dot{e}_i + \Lambda e_i \end{aligned} \tag{10}$$

Now the control objective is to design the torque input τ_i to restrict r_i to lie on the sliding surface (Slotine and Li 1987), so that the coupled errors e_i and $\dot{e}_i$ tend to zero. For easy implementation, the torque control input is ideally designed in a decentralized architecture.

To avoid the usage of dynamic modeling parameters, positive feedforward control gains are used in the controller formulation, i.e., K_i^H for $\dot{u}_i$ and K_i^C for u_i. To compensate for the effect due to the errors between these feedforward control gains and the actual dynamic models, a saturated control utilizing the *sign* function is utilized, in a similar manner to Utkin (1977) and Slotine and Sastry (1983). For simple implementation, each joint control only considers the synchronization between this joint and its two neighbor ones but not all others. Further, such a synchronization control would not affect the stability of the whole system.

Finally, the controller is designed as follows:

$$\begin{aligned} \tau_i = {} & K_i^H s_i^{-1} (\dot{u}_i - \dot{s}_i \dot{q}_i) + K_i^C s_i^{-1} u_i + K_{ri} s_i^{-1} r_i + \\ & sign\left(s_i^{-1} r_i\right) K_i^N + s_i^T K_\varepsilon (\varepsilon_i - \varepsilon_{i-1}) \end{aligned} \tag{11}$$

where K_i^H and K_i^C are positive feedforward control gains, K_{ri} and K_ε are positive feedback control gains, and K_i^N is a positive parameter that satisfies

$$K_i^N = \Delta_i^H \left\| s_i^{-1} (\dot{u}_i - \dot{s}_i \dot{q}_i) \right\| + \Delta_i^C \left\| s_i^{-1} u_i \right\| \tag{12}$$

In (12) Δ_i^H and Δ_i^C are scalars, whose selection will be discussed later. It is obvious to see that this controller formulation does not explicitly use the dynamic modeling parameters, and utilizes the information of the position errors of two neighbor joints. The *sign* function in (11) is for a saturation control used to compensate for the nonlinear effect caused by the error between the feedforward control gains and the modeling parameters, which was used in Utkin (1977) and Slotine and Sastry (1983) with stability analysis. From a theoretical viewpoint, Fillippov's (1988) inclusions may be used to properly address the issue in using the *sign* function. This approach, however, is not included in this paper. The last term in (11) is used to compensate for the effect of introducing the cross-coupling control on the overall system dynamics, which is required by the stability analysis.

It appears that parameters β and K_ε will dominate the control of the synchronization error. β plays a major role to reduce the synchronization error, while K_ε ensures the stability of the system when adding the cross-coupling control with β on the overall system dynamics.

Two assumptions are introduced:

ASSUMPTION 1. q_i^d and its first- and second-order derivatives are bounded.

ASSUMPTION 2. $H_i(q_i)$ and $C_i(q_i, \dot{q}_i)$ are bounded if their arguments are bounded.

Note that if $H_i(q_i)$ is time-varying, assumption 2 holds locally, i.e., Coriolis and centripetal forces are bounded by the square of the velocity norm.

A control gain tuning strategy is proposed as follows. First, select $\beta = 0$ and $K_\varepsilon = 0$, and tune the control gains K_i^H, K_i^C and K_{ri} using a trial and error method. The controller at this time is a normal feedforward/feedback control plus a saturation control without coupling. Second, gradually increase β from zero to introduce the synchronization control. As is seen in (7), the value of β determines the weight of the synchronization error ε_i in the coupled position error e_i, and thus affects the synchronization effort in the whole control action. Meanwhile, the control gain K_ε is also increased from zero, since it will be used to compensate for the effect of the introduction of the cross-coupling control due to β. Finally, the previously tuned gains may need to be changed slightly, utilizing a trial and error method.

Substituting (11) into the system dynamic equation yields the closed-loop dynamics:

$$\begin{aligned} &H_i(q_i)s_i^{-1}\dot{r}_i + C_i(q_i,\dot{q}_i)s_i^{-1}r_i + K_{ri}s_i^{-1}r_i + N_i \\ &sign\left(s_i^{-1}r_i\right)K_i^N + s_i^T K_\varepsilon(\varepsilon_i - \varepsilon_{i-1}) = 0 \end{aligned} \tag{13}$$

where

$$\begin{aligned} N_i = {} & (K_i^H - H_i(q_i))s_i^{-1}(\dot{u}_i - \dot{s}_i\dot{q}_i) \\ & + (K_i^C - C_i(q_i,\dot{q}_i))s_i^{-1}u_i \end{aligned} \tag{14}$$

THEOREM 1. The proposed tracking controller (11) leads to asymptotic stability of the system, namely, $\Delta q_i \to 0$ and $\varepsilon \to 0$ as time $t \to \infty$, under the conditions:

1. The scalars Δ_i^H and Δ_i^C are large enough to satisfy $\Delta_i^H \geqslant ||K_i^H - H_i(q_i)||$ and $\Delta_i^C \geqslant ||K_i^C - C_i(q_i,\dot{q}_i)||$.
2. The control gain K_{ri} is large enough to satisfy
$$\lambda_{\min}(K_{ri}) \geqslant \lambda_{\max}\left(H_i(q_i)\dot{s}_i^{-1}s_i\right)$$
where $\lambda_{\min}(\cdot)$ and $\lambda_{\max}(\cdot)$ denote the minimum and maximum eigenvalues of the matrices.

Proof. Define a Lyapunov function candidate as

$$\begin{aligned} V = {} & \sum_{i=1}^n \left[\tfrac{1}{2}r_i^T s_i^{-T} H_i(q_i)s_i^{-1}r_i + \tfrac{1}{2}\varepsilon_i^T K_{\varepsilon i}\varepsilon_i\right] + \\ & \tfrac{1}{2}\left(\int_0^t \sum_{i=1}^n(\varepsilon_i - \varepsilon_{i-1})dw\right)^T \Lambda\beta K_\varepsilon \left(\int_0^t \sum_{i=1}^n(\varepsilon_i - \varepsilon_{i-1})dw\right) \end{aligned} \tag{15}$$

Differentiating V with respect to time yields

$$\begin{aligned} \dot{V} = {} & \sum_{i=1}^n \begin{bmatrix} r_i^T s_i^{-T} H_i(q_i)s_i^{-1}\dot{r}_i + r_i^T s_i^{-T} H_i\dot{s}_i^{-1}r_i + \\ \tfrac{1}{2}r_i^T s_i^{-T}\dot{H}_i(q_i)s_i^{-1}r_i + \varepsilon_i^T K_{\varepsilon i}\dot{\varepsilon}_i \end{bmatrix} + \\ & \sum_{i=1}^n(\varepsilon_i - \varepsilon_{i-1})^T \Lambda\beta K_\varepsilon \int_0^t \sum_{i=1}^n(\varepsilon_i - \varepsilon_{i-1})dw \end{aligned} \tag{16}$$

Multiplying both sides of (13) by $\left(s_i^{-1}r_i\right)^T$ yields

$$\begin{aligned} &\left(s_i^{-1}r_i\right)^T H_i(q_i)s_i^{-1}\dot{r}_i + \left(s_i^{-1}r_i\right)^T C_i(q,\dot{q})s_i^{-1}r_i + \\ &\left(s_i^{-1}r_i\right)^T K_{ri}s_i^{-1}r_i + \left(s_i^{-1}r_i\right)^T N_i + \left\|s_i^{-1}r_i\right\| K_i^N + \\ &r_i^T K_\varepsilon(\varepsilon_i - \varepsilon_{i-1}) = 0 \end{aligned} \tag{17}$$

Substituting (17) into (16) yields

$$\begin{aligned} \dot{V} = {} & -\sum_{i=1}^n\left[\left(s_i^{-1}r_i\right)^T\left(K_{ri} - H_i(q_i)\dot{s}_i^{-1}s_i\right)s_i^{-1}r_i\right] \\ & -\sum_{i=1}^n\left[\left(s_i^{-1}r_i\right)^T N_i + \left\|s_i^{-1}r_i\right\| K_i^N\right] \\ & -\sum_{i=1}^n\left[r_i^T K_\varepsilon(\varepsilon_i - \varepsilon_{i-1})\right] + \sum_{i=1}^n \varepsilon_i^T K_\varepsilon\dot{\varepsilon}_i \\ & +\sum_{i=1}^n(\varepsilon_i - \varepsilon_{i-1})^T \Lambda\beta K_\varepsilon \int_0^t \sum_{i=1}^n(\varepsilon_i - \varepsilon_{i-1})dw \end{aligned} \tag{18}$$

Under condition 1 of Theorem 1, we have

$$\begin{aligned} & \left(s_i^{-1}r_i\right)^T N_i + \left\|s_i^{-1}r_i\right\| K_i^N \\ & \geqslant \left\|s_i^{-1}r_i\right\|\left(K_i^N - \|N_i\|\right) \\ = {} & \left\|s_i^{-1}r_i\right\|\left(\Delta_i^H\left\|s_i^{-1}(\dot{u}_i - \dot{s}_i\dot{q}_i)\right\| + \Delta_i^C\left\|s_i^{-1}u_i\right\| - \|N_i\|\right) \\ \geqslant {} & \left\|s_i^{-1}r_i\right\|\begin{pmatrix} \left\|K_i^H - H_i(q_i)\right\|\left\|s_i^{-1}(\dot{u}_i - \dot{s}_i\dot{q}_i)\right\| + \\ \left\|K_i^C - C_i(q_i,\dot{q}_i)\right\|\left\|s_i^{-1}u_i\right\| - \|N_i\| \end{pmatrix} \\ \geqslant {} & \left\|s_i^{-1}r_i\right\|\left(\left\|\begin{matrix} \left(K_i^H - H_i(q_i)\right)s_i^{-1}(\dot{u}_i - \dot{s}_i\dot{q}_i) + \\ \left(K_i^C - C_i(q_i,\dot{q}_i)\right)s_i^{-1}u_i \end{matrix}\right\| - \|N_i\|\right) \\ & = 0 \end{aligned} \tag{19}$$

We now analyze the term $\sum_{i=1}^{n}\left[r_i^T K_\varepsilon(\varepsilon_i-\varepsilon_{i-1})\right]$. From (6)–(10), we have

$$\begin{aligned}&\sum_{i=1}^{n} r_i^T K_\varepsilon(\varepsilon_i-\varepsilon_{i-1})\\&=\sum_{i=1}^{n}(r_i-r_{i+1})^T K_\varepsilon\varepsilon_i\\&=\sum_{i=1}^{n}\begin{bmatrix}\dot{\varepsilon}_i+\beta(2\varepsilon_i-\varepsilon_{i-1}-\varepsilon_{i+1})+\Lambda\varepsilon_i+\\ \Lambda\beta\int_0^t(2\varepsilon_i-\varepsilon_{i-1}-\varepsilon_{i+1})\,dw\end{bmatrix}^T K_\varepsilon\varepsilon_i\\&=\sum_{i=1}^{n}\dot{\varepsilon}_i^T K_\varepsilon\varepsilon_i+\sum_{i=1}^{n}\varepsilon_i^T\Lambda K_\varepsilon\varepsilon_i+\sum_{i=1}^{n}(\varepsilon_i-\varepsilon_{i+1})^T\beta K_\varepsilon\\&\sum_{i=1}^{n}(\varepsilon_i-\varepsilon_{i+1})+\sum_{i=1}^{n}(\varepsilon_i-\varepsilon_{i+1})^T\Lambda\beta K_\varepsilon\int_0^t\sum_{i=1}^{n}(\varepsilon_i-\varepsilon_{i+1})dw\end{aligned}\tag{20}$$

Substituting (19) and (20) into (18) and utilizing condition 2 of Theorem 1, we have

$$\begin{aligned}\dot{V}\leqslant&-\sum_{i=1}^{n}\left[\left(s_i^{-1}r_i\right)^T\left(\lambda_{\min}(K_{ri})-\lambda_{\max}\left(H_i(q_i)\dot{s}_i^{-1}s_i\right)\right)s_i^{-1}r_i\right]\\&-\sum_{i=1}^{n}\varepsilon_i^T\Lambda\beta K_\varepsilon\varepsilon_i-\sum_{i=1}^{n}(\varepsilon_i-\varepsilon_{i+1})^T\beta K_\varepsilon\sum_{i=1}^{n}(\varepsilon_i-\varepsilon_{i+1})\\&\leqslant 0\end{aligned}\tag{21}$$

Therefore, $r_i\to 0$ and $\varepsilon_i\to 0$ as time $t\to\infty$. The synchronization goal (5) is achieved. From (10), we further have $e_i\to 0$.

We now prove $\Delta q_i=0$ when $e_i=0$ and $\varepsilon_i=0$. Combining all equations in (7) from i to n, we have

$$s_1\Delta q_1+s_2\Delta q_2+\cdots+s_n\Delta q_n=0\tag{22}$$

Substituting (5) into (22) yields

$$s_1\Delta q_1=s_2\Delta q_2=\cdots=s_n\Delta q_n=0$$

Since s_i is not zero, $\Delta q_i=0$. Therefore, the system is asymptotically stable. □

Note that in the controller (13), the function $sign(\cdot)$ may cause chattering. To avoid this problem, we can use the function $\tan\mathrm{h}(\cdot)$ instead of $sign(\cdot)$ in a practical controller implementation.

4. Experiments

Experiments were performed on a three-DOF parallel manipulator, as shown in Figure 2, to evaluate the effectiveness of the proposed synchronous tracking controller. The control system of the parallel manipulator consists of a 400 Mhz Pentium II PC, a MCX-DSP-ISA 120Mflop/s DSP controller, and three Aerotech BA20 SineDrive amplifiers. The movable platform is actuated by three Aerotech BM200 DC brushless motors via THK KR3306 ball-screws each with a pitch of 6 mm. Built-in rotary encoder on the DC motor feeds back the angular position.

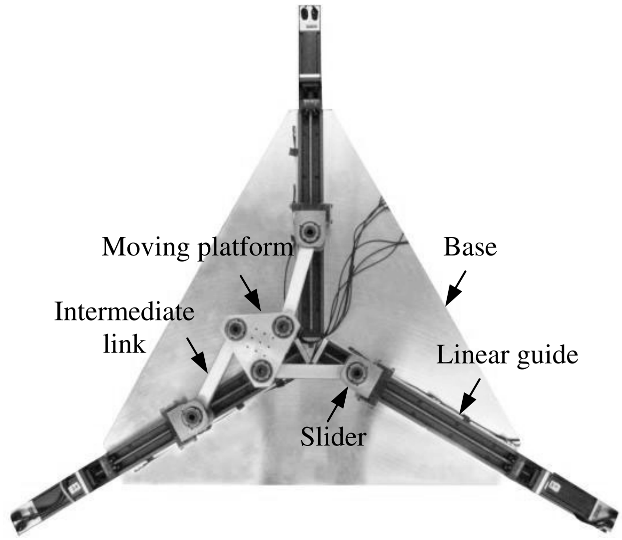

Fig. 2. Experimental setup of the parallel manipulator.

In the experiment, the synchronization function was designed in the same way as Su et al. (2006), namely

$$\frac{q_1(t)}{q_1^d(t)}=\frac{q_2(t)}{q_2^d(t)}=\cdots\frac{q_n(t)}{q_n^d(t)}\tag{23}$$

The rationale behind this goal is the observation that, when all ratios in (23) are equal, the manipulator moves in a synchronous manner. Hence, synchronization is achieved and the desired attitude of the movable platform is attained.

Then, following eq. (3), we have $s_i=\frac{1}{q_i^d(t)}$. It is necessary that all $q_i^d(t)$ be nonzero values during the entire motion. Due to singularities of the robot, the workspace of the robot (looks like a circle (Heerah and Behabib 2003)) was divided into six fan-shape areas with a common vertex at the centre of the circle. In addition, in order to study the control effect better, the size of the desired trajectory of the moving platform was selected as large as possible. As a result, the desired trajectory was selected as a triangular shape, which was as large as possible according to the limitation imposed by the size of the workspace of the moving platform.

Figure 3 illustrates the desired triangular path along which the platform was required to move. The attitudes of the platform at three vertexes were selected as: (5 mm, 5 mm, 44.3°), (45 mm, 70 mm, 44.3°) and (60 mm, 30 mm, 42.3°). The platform started and ended its motion at (5 mm, 5 mm, 44.3°), which is not at the origin to ensure that $q_i^d(t)$ are not zero. During the tracking, the maximum speed and accelerations were 0.3 m/s and 100 m/s^2, respectively. Note that the platform was in continuous motion between set points. Figure 4 illustrates the desired position trajectories of the prismatic joints.

For comparison purposes, three control algorithms including the proposed synchronous control, adaptive control

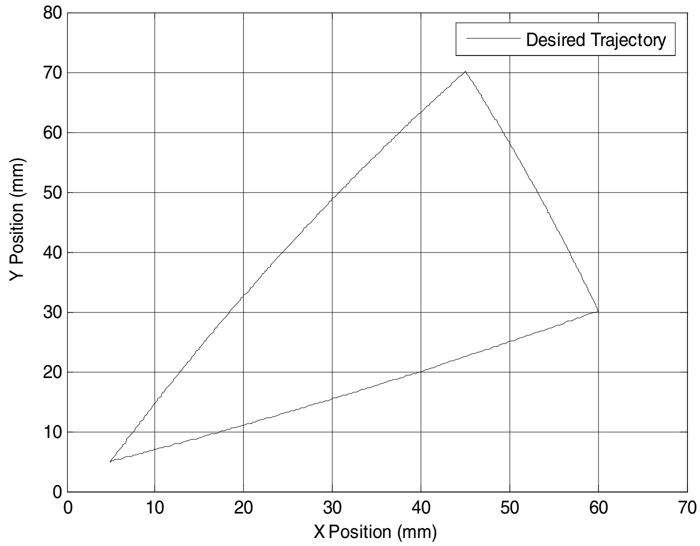

Fig. 3. Desired trajectory of the platform.

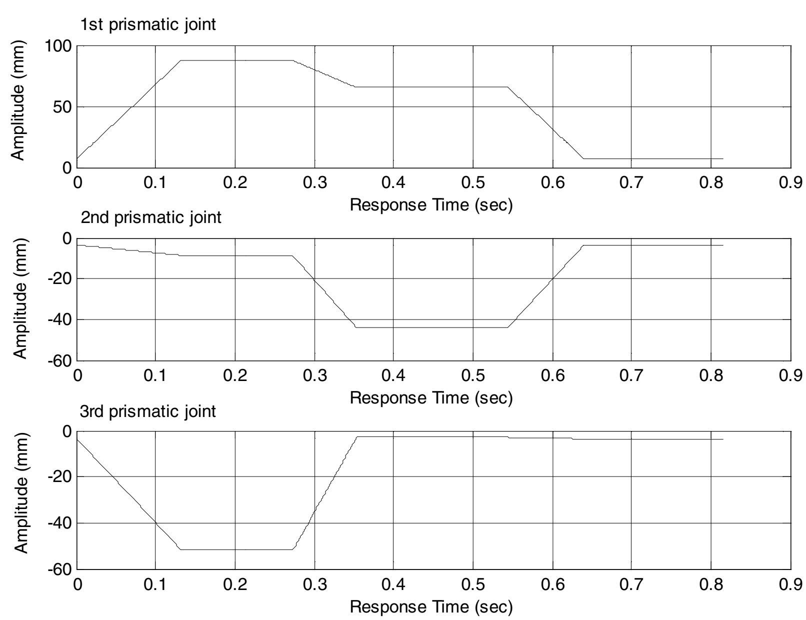

Fig. 4. Desired position trajectories of the prismatic joints.

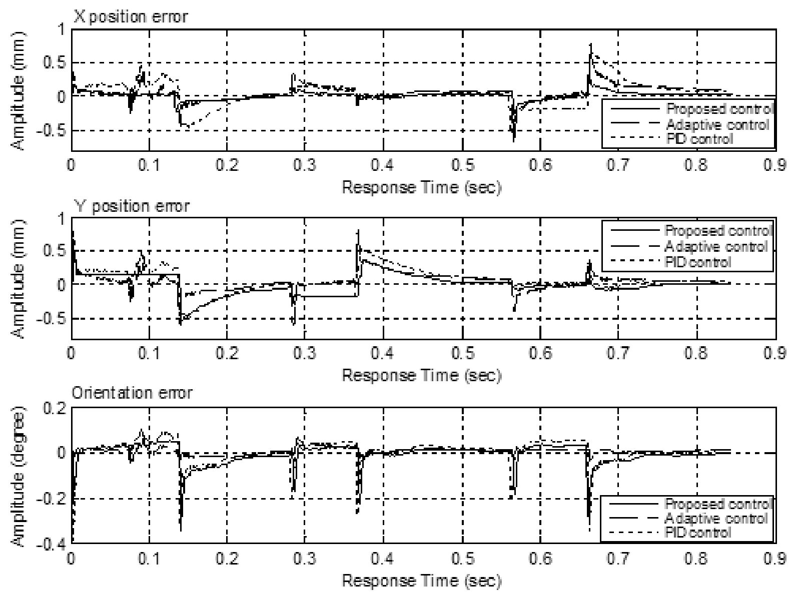

Fig. 5. Attitude errors of the platform with the three controllers.

(Slotine and Li 1987), and traditional PID control, were used to control the system respectively. The adaptive control (Slotine and Li 1987) is expressed as follows:

$$t_a = Y(q, \dot{q}, \ddot{q})\hat{\theta}(t) - K_a s(t) \tag{24}$$

The adaptation law is

$$\dot{\hat{\theta}}(t) = -PY(q, \dot{q}, \ddot{q})^T s(t) \tag{25}$$

where $K_a \in \Re^{3\times3}$ is a positive-definite diagonal gain matrix; $P \in \Re^{3\times3}$ is the positive-definite diagonal gain matrix of the estimator; both K_a and P are constant; $s(t) = \dot{e}(t) + \Lambda e(t)$, where $\Lambda \in \Re^{3\times3}$ is a positive-definite diagonal matrix.

Table 1 lists the selected control gains of the three control algorithms used in the experiments.

Figures 5 and 6 illustrate the attitude error of the platform and the position errors of the three prismatic joints, using the three control algorithms, where the solid lines denote the experimental results with the proposed synchronous control, the dashdot lines denote the results with the adaptive control, and the dotted lines denote the results with the PID control. The synchronization errors are shown in Figure 7. Table 2 gives a summary of the maximum absolute attitude errors of the platform and the maximum absolute position errors of the three prismatic joints using the three controllers during the tracking motions. It can be seen through comparison of these results, that the synchronous control exhibits faster convergence speed, smaller position errors of the prismatic joints,

Table 1. Control Gains of the Four Controllers

Controllers	Control Gains
Proposed control	$\alpha = 0.21$, $\beta = 0.15$, $\Delta^H = 0.013$, $\Delta^C = 1.2$, $\Lambda = \{0.06\}$, $K^H = diag\{0.014\}$ $K^C = diag\{1.6\}$, $K_r = diag\{0.002\}$, $K_\varepsilon = diag\{0.01\}$, $K_N = diag\{1.4\}$
Adaptive control	$\Lambda = \{0.8\}$, $K_a = diag\{1.8\}$
PID control	$K_p = diag\{2\}$, $K_i = diag\{1.4\}$, $K_d = diag\{0.016\}$

and smaller attitude error of the platform, compared to the other two control methods. In other words, the synchronous control improves the trajectory tracking performance indeed.

5. Conclusions

In this paper, a cross-coupling control approach is proposed for synchronous control of parallel manipulators. The controller utilizes feedback of position synchronization errors, which are defined as differential position errors between two adjacent actuator joints. The controller has the form of feed-

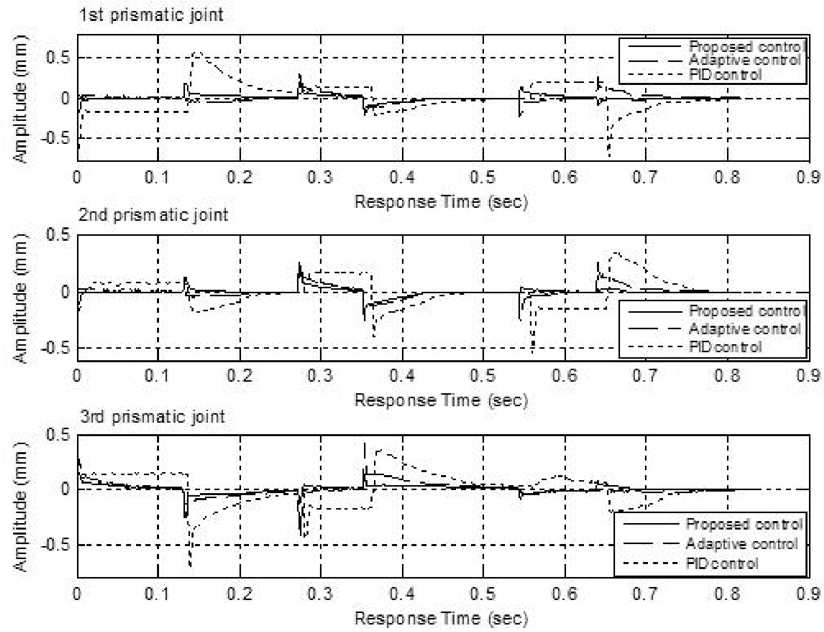

Fig. 6. Prismatic joint position errors with the three controllers.

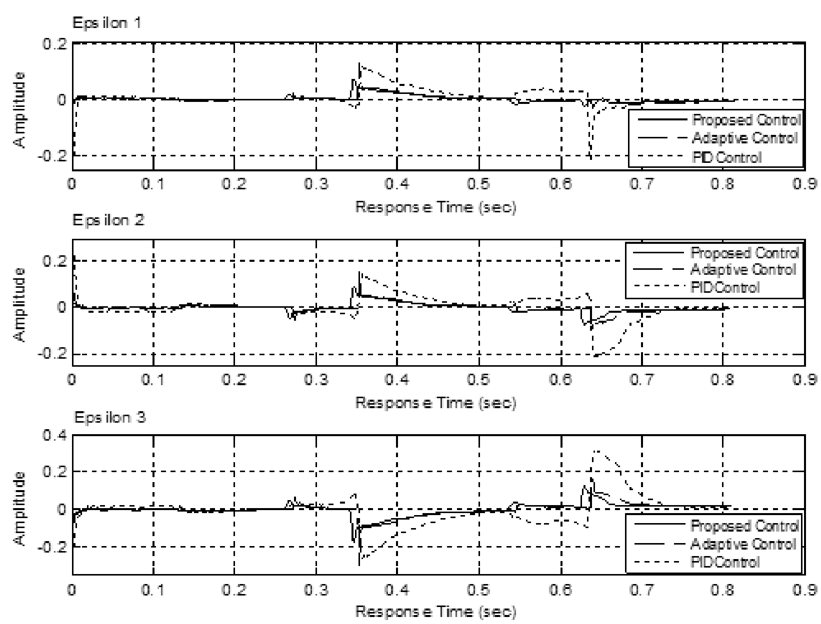

Fig. 7. Synchronization errors of the three controllers.

Table 2. Maximum Absolute Errors

Maximum Absolute Errors	Adaptive PID	Synchronous Control	Control
X Position error of platform (mm)	0.679	0.672	0.412
Y Position error of platform (mm)	0.818	0.810	0.376
Orientation error of platform (deg)	0.393	0.070	0.058
1^{st} prismatic joint error (mm)	0.755	0.423	0.198
2^{nd} prismatic joint error (mm)	0.502	0.290	0.219
3^{rd} prismatic joint error (mm)	0.717	0.417	0.285
Synchronization error ε_1	0.2166	0.1322	0.0726
Synchronization error ε_2	0.2681	0.1578	0.0909
Synchronization error ε_3	0.3181	0.2986	0.1695

forward/feedback control plus a saturation control. It is proved that the proposed synchronous controller leads to asymptotic convergence to zero of both position and synchronization errors. The effect of cross-coupling on system stability has been investigated. The major advantage of the proposed method lies in: (1) performance improvement through synchronous control of actuators; (2) no explicit use of the system dynamic model. Experiments conducted on a 3-DOF parallel manipulator system verify the effectiveness of the performance improvement through synchronous control of actuators.

Acknowledgment

This work was partly supported by a grant from Research Grants Council of the Hong Kong Special Administrative Region, China under grant CityU 119705, and a grant from City University of Hong Kong under project 7001923.

References

Amirat, Y., Francois, G. F., Pontnau, J. and Dafaoui, M. 1996. Design and control of a new six DOF parallel robot: Application to equestrian gait simulation, *Mechatronics International Journal of Mechanics, Electronics and Control* 6(2):227–239.

Angeles, J. and Lee, S. K. 1989. The modeling of holonomic mechanical systems using a natural orthogonal complement, *Transactions CSME* 13(4):81–89.

Begon, P., Pierrot, F., and Dauchez, P. 1995. Fuzzy sliding mode control of a fast parallel robot, in *Proceedings of IEEE International Conference on. Robotics and Automation.*, pp.1178–1183.

Borenstein, J. and Koren, Y. 1987. Motion control analysis of a mobile robot, *ASME Journal of Dynamic Systems, Measurement and Control* 109:73–79.

Borenstein, J. Feb. 1995. Control and kinematic design of multi–degree–of freedom mobile robots with compliant linkage, *IEEE Transactions on Robotics and Automation* 11:21–35.

Carretero, J. A., Nahon, M., and Podhorodeski, R. P. 1998. Workspace analysis of a 3–DOF parallel mechanism, *Proceedings of IEEE International Conference on Intelligent Robots and Systems*, vol. 2, pp. 1021–1026.

Chen, N. X. and Song, S. 1994. Direct position analysis of 4-6 Stewart Platforms, *Journal of Mechanical Design* 116:61–66.

Chiacchio, P., Pierrot, F., Sciavicco, L. and Siciliano, B. 1993. Robust Design of independent joint controllers with experimentation on a high–speed parallel robot, *IEEE Transactions Industrial Electronics*, 40(4):393–403.

Chiu, T. C. and Tomizuka, M. 1998. Coordinated position control of multi–axis mechanical systems. *ASME Journal of Dynamic Systems, Measurement, and Control* 120(3):389–393.

Chiu, T. C., and Tomizuka, M. 2001. Contouring control of machine tool feed drive systems: A task coordinate frame approach, *IEEE Transactions on Control Systems Technology* 9(1):130–139.

Chuang, H.-Y. and Chang, Y.-C. 2000. A novel contour error compensator for 3–PRPS platform, *Journal of Robotic Systems* 17(5):273–289.

Clavel, R. 1998. Delta, a fast robot with parallel geometry, *Proceedings 18th International Symposium on Industrial Robots*, Lausanne, Switzerland, pp. 91–100.

Fasse, E. D. and Gosselin, C. M. 1999. Spatio–geometric impedance control of Gough–Stewart platforms, *IEEE Transaction on Robotics and Automation* 15:281–288.

Feng, L., Koren, Y. and Borenstein, J. 1993. Cross–coupling motion controller for mobile robots, *IEEE Control Sysems. Magazine* 13(6):35–43.

Filippov, A. F. 1988. *Differential Equations with Discontinuous Righthand Sides*, Kluwer, Dordrecht.

Gauthier, D., Freeman, P., Carayannis, G. and Malowany, A. 1987. Interprocess communication for distributed robotics. *IEEE Transactions on Robotics and Automation* 3(6): 493–504.

Heerah, I. and Behabib, B. 2003. Architecture selection and singularity analysis of a three–degree–of–freedom planar parallel manipulator, *Journal of Intelligent and Robotic Systems* 37:355–374.

Kamano, T., Suzuki, T., Iuchi, N. and Tomizuka, M. 1993. Adaptive feedforward controller for synchronization of two axes positioning system. *Transactions of Society of Instrument and Control Engineers* (SICE), Japan, 29(7):785–791.

Karkoub, M., Her, M. G., Hsu, K. S. and Chen, C. Y. 2004. Neural–net tuned PID control of a parallel type mechanism with force feedback for virtual reality applications, *Robotica* 22(3):319–327.

Kokkinis, T. and Stoughton, R. 1996. Dynamics and control of closed–chain robot arms with application to a new direct–drive robot arm, *Inernational Journal of Robotics and Automation*, 6(1):25–34.

Koren, Y. 1980. Cross–coupled biaxial computer controls for manufacturing systems, *ASME Journal of Dynamic Systems, Measurement,and Control* 102(4):265–272.

Koren, Y. and Lo, C. C. 1991. Variable–gain cross–coupling controller for contouring, *Annals of CIRP* 40(1):371–374.

Koren, Y. and Lo, C. C. June 1992. Evaluation of servo–controllers for machine tools, *Proceedings of American Control Conference*, pp. 370–374.

Koren, Y. and Lo, C. C. 1992. Advanced controllers for feed drives. *Annals of CIRP* pp. 689–698.

Kulkarni P. K. and Srinivasan, K. 1990. Cross–coupled control of biaxial feed drive servomechanisms, *ASME Journal of Dynamic Systems, Measurement,and Control* 112(2):225–232.

Lee, H. C. and Jeon, G. J. 1998. A neuro–controller for synchronization of two motion axes, *International Journal of Intelligent Systems* 13(6):571–586.

Li, S., Feng, Z. and Fang, H. 2002. Variable structure control for 6–6 parallel manipulators based on cascaded CMAC, *Proceedings of 4th World Congress on Intelligent Control and Automations*, Shanghai, China, pp. 1939–1943.

Lin, H. M. and McInroy, J. E. 2003. Adaptive sinusoidal disturbance cancellation for precise pointing of Stewart platforms, *IEEE Transactions on Control Systems Technology* 11:267–272.

Merlet, J. P. 2000. *Parallel Robots*, Kluwer Academic Publishers, Dordrecht, pp. 9–10.

Moore, P. R. and Chen, C. M. 1995. Fuzzy logic coupling and synchronized control of multiple independent servo–drives, *Control Engineering Practice* 3(12):1697–1708.

McNab, R. and Tsao, T. November 1994. Multiaxis contour tracking: A receding time horizon linear quadratic optimal control approach, *Dynamic System and Control* 2.

McNab, R. J. and Tsao, T. C. 2000. Receding horizon linear quadratic optimal control for multi–axis contour tracking. *ASME Journal of Dynamic Systems, Measurement, and Control* 122(2):375–381.

Naumovic, M. 1999. Cross–coupled motion controller for two cooperating robot arms, in *Proceedings of IEEE International Symposium on Industrial Electronics*, vol. 2, pp. 909–913.

Nefti, S., Djouani, K. and Amirat, Y. 2002. Neuro–fuzzy based approach for hybrid force/position robot control, *Proceedings of IEEE International Conference on Industrial Technology*, Bangkok, Thailand, pp. 376–381.

Park, M. K., Lee, M. C. and Go, S. J. 2001. The design of sliding mode controller with perturbation observer for a 6–DOF parallel manipulator, *Proceedings of International Symposium on Industrial Engineering*, Pusan, Korea, vol. 3, pp. 1502–1507.

Pernechele, C., Bortoletto, F. and Giro, E. 2000. Neural network algorithm controlling a hexapod platform, in *Proceedings of IEEE–INNS–ENNS International Joint Conference on Neural Networks*, pp. 349–352.

Rodriguez–Angeles, A. and Nijmeijer, H. 2004. Mutual synchronization of robots via estimated state feedback: A cooperative approach, *IEEE Transactions on Control Systems Technology* 12:542–554.

Sirouspour, M. R. and Salcudean, S. E. 2001. Nonlinear control of hydraulic robots, *IEEE Transactions on Robotics and Automation* 17:173–182.

Slotine, J. J. E. and Li, W. 1987. On the adaptive control of robot manipulators, *International Journal of Robotics Research* 6(3):49–59.

Slotine, J. J. E. and Sastry, S. 1983. Tracking control of nonlinear systems using sliding surfaces, with application to robot manipulators, *International Journal of Control* 38:465–492.

Stauffer, R. N. 1984. Flight simulation facility features robot position, *Robotics Today* 6(3):71–72.

Su, Y. X., Sun, D., Ren, L. and Mills, J. K. 2006. Integration of saturated PI synchronous control and PD feedback for control of parallel manipulators, *IEEE Transactions on Robotics* 22(1):202–207.

Sun, D. 2003. Position synchronization of multiple motion axes with adaptive coupling control. *Automatica* 39(6):997–1005.

Sun, D., Feng, G., Lam, C. M. and Dong, H. N. 2005. Orientation control of a differential mobile robot through wheels' synchronization, *IEEE/ASME Transactions on Mechatronics* 10(3):345–351.

Sun, D. and Mills, J. K. 2002. Adaptive synchronized control for coordination of multirobot assembly tasks, *IEEE Transactions on Robotics and Automation* 18:498–510.

Tomizuka, M., Hu, J. S. and Chiu, T. C. 1992. Synchronization of two motion control axes under adaptive feedforward control, *ASME Journal of Dynamic Systems, Measurement,and Control* 114(6):196–203.

Utkin, V. I. 1977. Variable structure systems with sliding modes, *IEEE Transactions on Automatic Control* AC–22(2):212–222.

Yang, L. F. and Chang, W. H. 1996. Synchronization of twin–gyro precession under cross–coupled adaptive feedforward control. *Journal of Guidance, Control, and Dynamics* 19(3):534–539.

Yeh, S. S. and Hsu, P. L. 2003. Analysis and design of integrated control for multi–axis motion systems, *IEEE Transactions on. Control Systems Technology* 11:375–382.